J Ther Eng, Vol. 9, No. 3, pp. 602−613, May, 2023

Journal of Thermal Engineering
Web page info: https://jten.yildiz.edu.tr
DOI: 10.18186/thermal.1297545

Journal of Thermal Engineering

Research Article

Simulation of heat transfer and effectiveness in a helical heat exchanger made from thermally enhanced polymer material for use in absorption cooling

Talib AHMADU[1,*], Hamisu Adamu DANDAJEH[1]

[1]*Department of Mechanical Engineering, Faculty of Engineering, Ahmadu Bello University, Zaria, 810107, Nigeria*

ARTICLE INFO

Article history
Received: 01 June 2021
Accepted: 01 October 2021

Keywords:
Modelling; Helical Heat Exchanger; Thermally Enhanced Polymer; Absorption Chiller

ABSTRACT

Heat exchangers in absorption chillers are usually made of copper material. However, problems of corrosion are usually encountered, especially in the solution heat exchanger. In this study a numerical investigation of the heat transfer effectiveness in a double pipe helical heat exchanger made from a thermally enhanced polymer material was conducted. The material consists of a Liquid crystal polymer (LCP), (Vectra A950) as the matrix material, while carbon fibre is the filler material. The resulting composite has a carbon fibre weight fraction of 74%. The heat exchanger was modelled as a counter flow solution heat exchanger to be used in a lithium bromide – water absorption chiller of 3 kW capacity. The numerical software ANSYS fluent (version 14.5) was used for the modelling and simulation. Thermal and mechanical properties of the thermally enhanced polymer were used in the modelling and simulation. The viscous laminar model was used, while employing a second order upwind solution method. Results indicate that the heat exchanger was able to perform the required duty by reducing the strong solution temperature from 90°C at inlet to 57°C at outlet, while increasing the weak solution temperature from 40°C at inlet to 67°C at outlet. The effectiveness of the heat exchanger was 77.4%. Results were numerically compared to a corresponding heat exchanger of same geometry and flow conditions, made of copper. It was observed that the polymer heat exchanger attained 89.2% effectiveness of the copper heat exchanger.

Cite this article as: Ahmadu T, Dandajeh HA. Simulation of heat transfer and effectiveness in a helical heat exchanger made from thermally enhanced polymer material for use in absorption cooling. J Ther Eng 2023;9(3):602−613.

INTRODUCTION

Heat exchangers are devices that facilitate the transfer of heat from one fluid medium across a solid boundary to another fluid medium. In air – conditioning, refrigeration and energy recovery applications, heat exchangers are very important to the overall efficiency, cost and size of the system [1]. Current heat exchanger designs rely heavily on shell and tube or plate heat exchangers, often constructed using copper, stainless steel and aluminium. In absorption chillers, the major components: Generator, Condenser,

*Corresponding author.
*E-mail address: talibahmadu@gmail.com

This paper was recommended for publication in revised form by Regional Editor Ahmet Selim Dalkılıç

Published by Yıldız Technical University Press, İstanbul, Turkey

Absorber, Evaporator and Solution Heat Exchanger are usually of the shell and tube heat exchanger type, constructed using copper or stainless steel. Parts constructed of copper, when in contact with lithium bromide solution are usually prone to corrosion [2].

Recently, helical heat exchangers have been widely adopted in process industries, including refrigeration equipment. This is as a result of the secondary flow induced by its curvature, smaller foot print and higher heat transfer rate [3]. Also, recent developments in material science, especially advances in polymers offer advantages for new heat exchanger designs and applications [4]. According to [5], polymers can be corrosion resistant to almost all chemicals. Polymer heat exchangers offer good anticorrosion and antifouling properties, they are also low in cost and weight [6].

Thermally enhanced polymers are filler loaded thermoplastics with the ultimate aim of enhancing their mechanical and thermal properties, notably the thermal conductivity [7]. They offer favourable qualities such as: good corrosion resistance, higher thermal conductivities, higher strengths, low embodied energy and good manufacturability, which makes them suitable for a variety of heat exchanger applications [4].

In order to have lithium bromide – water absorption chillers with good effectiveness, compactness and low corrosion problems, it has become imperative to employ heat exchanger designs that will ensure compactness, as well as use materials that are less susceptible to corrosion. A combination of helical heat exchanger design using thermally enhanced polymer material could ensure compactness, less corrosion problems and still maintain good effectiveness in lithium bromide – water absorption chillers. This forms the focus of the present work.

Research works are ongoing on the use of helical heat exchangers as well as thermally enhanced polymer materials in heat exchanger design for a variety of applications in mechanical refrigeration. A parametric thermo-fluid performance analysis of a conceptual double finned plate heat exchanger module was conducted [8]. They concluded that the thermal conductivities achievable for enhanced thermoplastics (within 20W/mK) can produce approximately half the heat transfer rate of an aluminium heat exchanger operating under the same conditions. Experimental evaluation of the heat transfer characteristics of a double pipe helical heat exchanger has been conducted [9]. Two differently sized heat exchangers were used. Flow rates in the inner and outer tubes were varied and fluid temperatures recorded. They observed that heat transfer rates were much higher in counter flow than parallel flow configuration. In a related study, numerical analysis of the laminar fluid flow and heat transfer characteristics of a double pipe helical heat exchanger under different flow rates and tube sizes, in both parallel and counter flow was done [10]. The results showed an increase in overall heat transfer coefficient as the inner Dean number increases. Performance of a shell and helical coil type solution heat exchanger in an ammonia – water vapour absorption system was evaluated experimentally [11]. A heat exchanger effectiveness of 0.84 – 0.9 was obtained for the tested conditions. Experimental and numerical investigation of heat transfer in a counter flow, double pipe helical heat exchanger has been done [12]. The inner tube was made of copper, while the outer tube was made of polypropylene random (PPR). The working fluid was water. Effect of circular grooves on helical heat exchanger effectiveness was investigated numerically [13]. Results indicated an increase in performance with the circular grooves. Multi – objective genetic algorithm was used by [14] to evaluate the performance of a helical heat exchanger. Commercial computational tool ANSYS was used by [15] to investigate the effect of Dean number on the heat transfer characteristics of a helical coil tube heat exchanger with variable velocity and pressure inlet. The working fluid was water. Results indicated that increase in Dean number increases the heat transfer of the heat exchanger.

Studies on polymer materials for heat exchanger in absorption chiller components are however limited. This study intends to carry out a Computational Fluid Dynamics (CFD) analysis of the heat transfer and effectiveness in a double pipe helical heat exchanger used as a solution heat exchanger in a lithium bromide – water absorption chiller unit. The heat exchanger is made from a thermally enhanced liquid crystal polymer (LCP) material.

THE ABSORPTION CHILLER AND SOLUTION HEAT EXCHANGER

The main components of the absorption chiller are as shown in Figure 1: Generator (G), Condenser (C), Absorber (A), Evaporator (E) and Solution Heat Exchanger (SHX). The solution heat exchanger facilitates heat transfer

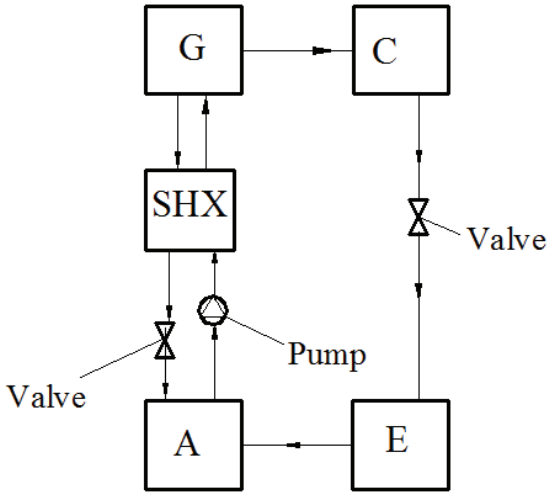

Figure 1. Schematic of a single effect absorption cooling cycle

between the high temperature strong solution from the generator and the low temperature weak solution from the absorber. This is to ensure that the strong solution on entry to the absorber is reduced in temperature to the absorber temperature so as to achieve a continuous absorption process. While on the other hand, the weak solution on entry to the generator is increased in temperature to a temperature close to the generator temperature to minimize the energy required to desorb the aqueous lithium bromide (LiBr) solution at the generator. It is this solution heat exchanger that we seek to replace with a double pipe helical heat exchanger using a LCP based thermally enhanced polymer material. The helical design of the solution heat exchanger is expected to reduce its size. Also, using a LCP based thermally enhanced polymer will reduce chances of corrosion in the solution heat exchanger.

Double Pipe Helical Heat Exchanger

In order to overcome some of the problems associated with shell and tube heat exchanger, a double pipe helical heat exchanger is studied as the solution heat exchanger. This heat exchanger consists of one pipe placed concentrically inside another pipe having a greater diameter.

The curvature in the tubes creates a secondary flow, which is normal to the primary axial direction of flow. This secondary flow caused by centrifugal force, increases the heat transfer between the wall and the flowing fluid [16]. Also, the whole surface area of the coil is exposed to the moving fluid, eliminating the dead zones that could be found in shell and tube heat exchangers. They offer a great heat transfer area within a small space, high heat transfer coefficients as well as compactness. When constructed of a LCP based thermally enhanced polymer, the heat exchanger could also offer great resistance to corrosion. Fabrication of thermally enhanced polymer helical heat exchanger can be done via rapid prototyping. This technology will ensure design specifications are met and good surface finish achieved, leading to smooth pipes with minimal flow resistance.

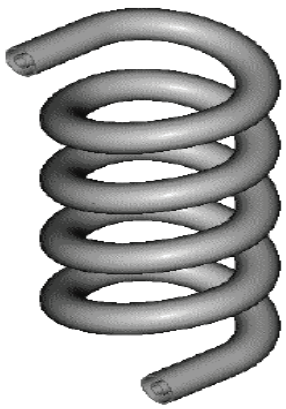

Figure 2. Schematic of a double pipe helical heat exchanger

METHODOLOGY

Design of the helical heat exchanger was done taking into consideration the required heat exchanger duty and the material to be used (thermally enhanced polymeric material). Modelling and CFD analysis were done using the numerical software ANSYS fluent.

Properties of the Thermally Enhanced Polymer Material

A commercially available thermally enhanced polymeric material was used as the material in modelling the helical heat exchanger. The material consists of a Liquid Crystal Polymer (Vectra A950) as the matrix material, while carbon fibre is the filler material. The resulting composite has a carbon fibre weight fraction of 74%. Thermal and mechanical properties of the resulting thermally enhanced polymeric material are shown in table 1.

Table 1. Properties of the thermally enhanced polymeric material [8]

Property	Value
Thermal conductivity (W/mK)	20
Tensile strength (MPa)	103.4
Tensile modulus (GPa)	20.7
Density (g/ cc)	1.82
HDT at 1.8 MPa (°C)	277

Design of the Helical Heat Exchanger

Table 2 shows the summary of the heat exchanger design parameters

Table 2. Summary of Heat Exchanger Design parameters

Design Parameter	Value
Chiller capacity (kW)	3
SHX duty (kW)	0.7
SHX configuration	Counter flow
Strong LiBr solution inlet temp. (°C) (Hot fluid)	90
Weak LiBr solution inlet temp. (°C) (Cold fluid)	40
Strong LiBr solution concentration	0.63
Weak LiBr solution concentration	0.55
Inner pipe inner dia. (m)	0.026
Outer pipe inner dia. (m)	0.05
Thickness of pipes (m)	0.004
Strong LiBr solution flow rate (kg/s)	0.0286
Weak LiBr solution flow rate (kg/s)	0.0244
Total heat exchanger length (m)	1.5
Number of turns	3
Coil radius (m)	0.08
Height of heat exchanger (m)	0.25
Required strong LiBr solution exit temp. (°C)	55
Required weak LiBr solution exit temp. (°C)	74

Heat Exchanger Performance Calculations

The total rate of heat transfer between the hot and cold fluids is calculated as [1]:

$$q = \dot{m}_h C_{p,h}\left(T_{h,i} - T_{h,o}\right) \quad (1)$$

$$\text{And } q = \dot{m}_c C_{p,c}\left(T_{c,o} - T_{c,i}\right) \quad (2)$$

The overall heat transfer coefficient is calculated as [1]:

$$U = \frac{q}{A\Delta T_{lm}} \quad (3)$$

$$\text{Where } \Delta T_{lm} = \frac{\Delta T_2 - \Delta T_1}{ln\left({}^{\Delta T_2}/_{\Delta T_1}\right)} \quad (4)$$

$$\text{Where } \Delta T_1 = T_{h,i} - T_{c,o} \quad (5)$$

$$\text{And } \Delta T_2 = T_{h,o} - T_{c,i} \quad (6)$$

The effectiveness of the heat exchanger is calculated as [1]:

$$\varepsilon = \frac{q}{q_{max}} \quad (7)$$

$$\text{Where } q_{max} = C_{min}\left(T_{h,i} - T_{c,i}\right) \quad (8)$$

Where C_{min} is equal to C_c or C_h, whichever is smaller.

C_c and C_h are the heat capacity rates of the cold fluid and hot fluid respectively, given as:

$$C_c = \dot{m}_c C_{p,c} \quad (9)$$

$$\text{and } C_h = \dot{m}_h C_{p,h} \quad (10)$$

The Dean number is calculated as [10]:

$$De = Re\sqrt{\frac{D_h}{2R_c}} \quad (11)$$

$$\text{Where } Re = \frac{\rho V D}{\mu} \quad (12)$$

$$\text{Also, } Re_{annuls} = \frac{\rho v(D_{io} - D_{oi})}{\mu} \quad (13)$$

Where Re_{annuls} is the Reynolds number at the annulus, D_{io} and D_{oi} are the inner diameter of the outer pipe and outer diameter of the inner pipe respectively.

The curvature in double pipe helical heat exchanger creates secondary flow. This contributes to delaying the transition from laminar to turbulent flow to a higher Reynolds number as compared to straight pipes [17]. The critical Reynolds number for the transition from laminar to turbulent flow in helical coil pipes is a function of the curvature ratio of the coil [17]. The correlation of [18] is used to compute the critical Reynolds number as:

$$Re_{crit} = 2100\left(1 + 12\sqrt{\frac{r}{R_c}}\right) \quad (14)$$

CFD Modelling

The numerical package ANSYS fluent (version 14.5) was used in the CFD modelling, simulation and analysis. A three-dimensional model of the helical heat exchanger was developed in the ANSYS workbench design module using the dimensions given in table 1. The mesh for the domain was constructed after which boundary and initial conditions were applied. A solution method was then applied to generate results.

Governing equations

The flow of fluid in curved tubes is governed by the continuity equation, the energy equation and the Navier-Stokes momentum equation given in equations 15, 16 and 17 respectively. The continuity and momentum equations are used to calculate the velocity vector, the energy equation is used to calculate temperature distribution, wall heat flux and wall heat transfer coefficient [19].

The continuity equation, valid for compressible or incompressible flow as given by [19] is as shown in equation 15:

$$\frac{\partial \rho}{\partial t} + \nabla.\left(\rho\vec{V}\right) \quad (15)$$

ANSYS fluent solves the energy equation in the following form as shown in equation 16:

$$\frac{\partial}{\partial t}(\rho E) + \nabla.\left(\vec{v}\,(\rho E + p)\right) = \nabla.\left(K_{eff}\nabla T - \sum_j h_j\overrightarrow{J_j} + \left(\bar{\bar{\tau}}_{eff}.\vec{v}\right)\right) + S_h \quad (16)$$

The first three terms on the right hand side of equation 15 represent the energy transfer due to conduction, species diffusion and viscous dissipation respectively. Where E is the total energy, ρ is the density and p is the pressure. S_h is the heat of chemical reaction and any other volumetric sources. K_{eff} is the effective conductivity, $\overrightarrow{J_J}$ is the diffusion flux of species J. $\bar{\bar{\tau}}_{eff}$ is the effective stress tensor, $\vec{v}$ is the velocity field, T is the temperature.

The Navier-Stokes momentum equation as given by [19] is as shown in equation 17:

$$\frac{\partial}{\partial t}(\rho\vec{v}) + \nabla.(\rho\vec{v}\vec{v}) = -\nabla p + \nabla.(\bar{\bar{\tau}}) + \rho\vec{g} + \vec{F} \quad (17)$$

Where ρ is the density, p is the static pressure, $\vec{v}$ is the velocity field, $\bar{\bar{\tau}}$ is the stress tensor, $\rho\vec{g}$ is the gravitational body force, $\vec{F}$ is the external body force.

Fluid settings

Fluid settings were done in ANSYS fluent using the properties of aqueous lithium bromide solution as contained in [20]. Mean operating temperatures and concentrations for the heat exchanger were used. The operating temperatures and concentrations are as given in table 2. Table 3 shows the fluid settings.

Table 3. Fluid settings

Property	Value
Density (kg/m^3)	1629
Dynamic viscosity (N.s/m^2)	0.002068
Thermal conductivity (W/mK)	570.7
Specific heat capacity (J/kgK)	2354.6

Solution procedure

Equation 14 along with the tube radius and coil radius as given in table 2, were used to compute the critical Reynolds number. The Reynolds number of flow in the inner tube and annulus were computed using equations 12 and 13 respectively. Properties of aqueous lithium bromide as given in table 3 were used to compute the Reynolds number of flow. The Reynolds number of flow, both in the tube and annulus were less than 2,100, an indication that the flow is in the laminar regime. Viscous laminar model was therefore used in the simulation.

Hybrid initialization method was applied for initializing the temperature and velocity fields in the computational domain. The semi implicit pressure linked equation (SIMPLE) algorithm was used to carry out pressure – velocity coupling. In order to achieve better accuracy, second-order upwind discretization was applied to the tetrahedral and hexahedral meshes in the computational domain. The boundary and initial conditions applied to the computational domain are the temperatures of the hot and cold lithium bromide solutions at inlet to the heat exchanger as well as the mass flow rates of the solutions. The values are as contained in table 2. Steady and incompressible flow was assumed. Changes in densities and specific heats of lithium bromide solutions were considered negligible.

Model validation

To validate the numerical model developed in this work, numerical simulations were compared with the works of [9]. This was done by adjusting the model to the same geometric, thermal and boundary conditions as used in the works of [9]. In their works, they used a counter flow configuration with uniform inlet conditions (mass flow rate and temperature), in the laminar regime. The fluid used was water and the material is stainless steel. Three ratios of flow rates of fluid at the annulus to that at the inner pipe of 0.5, 1 and 2 were used. Dean number was varied from 38 to 350 and the effect on the overall heat transfer coefficient obtained. Figure 3 shows the comparison of the results obtained from the simulations in the present work with those obtained in [9]. It can be seen from the figure that the results from the present work are in good agreement with those from [9] thus validating the developed numerical model.

RESULTS AND DISCUSSIONS

Figure 4 shows the three-dimensional model of the helical heat exchanger in ANSYS design modeler studio as well as close up view of the entrance region showing dimensions.

Figure 5 shows the generated mesh for the computational domain. The mesh is seen to consist of tetrahedral and hexahedral meshes. Table 4 shows the number of nodes

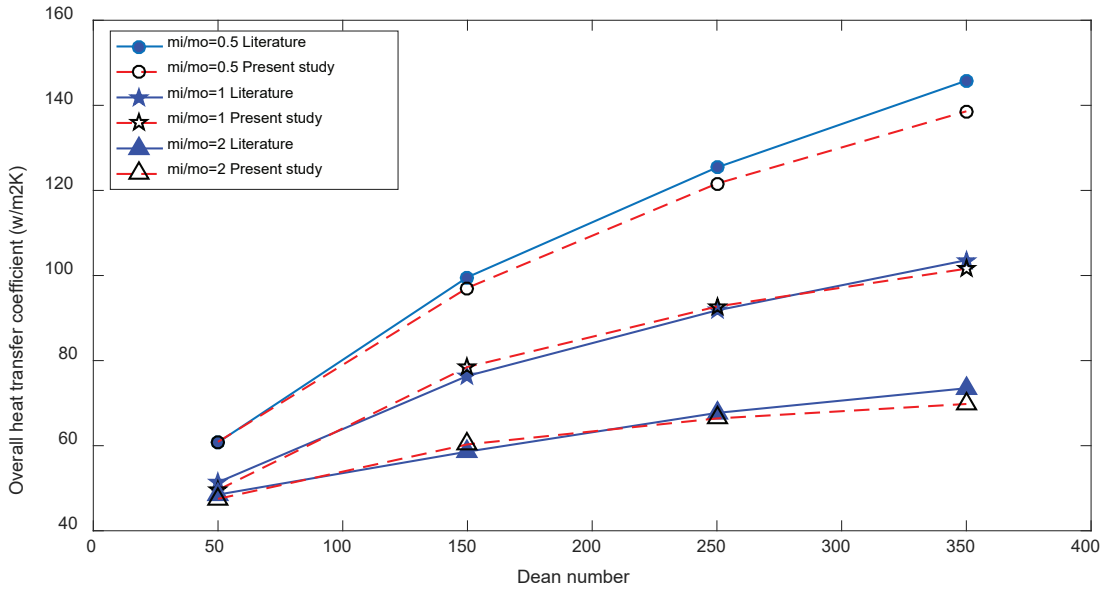

Figure 3. Comparison of variation of overall heat transfer coefficient with Dean number for present work with literature of [9].

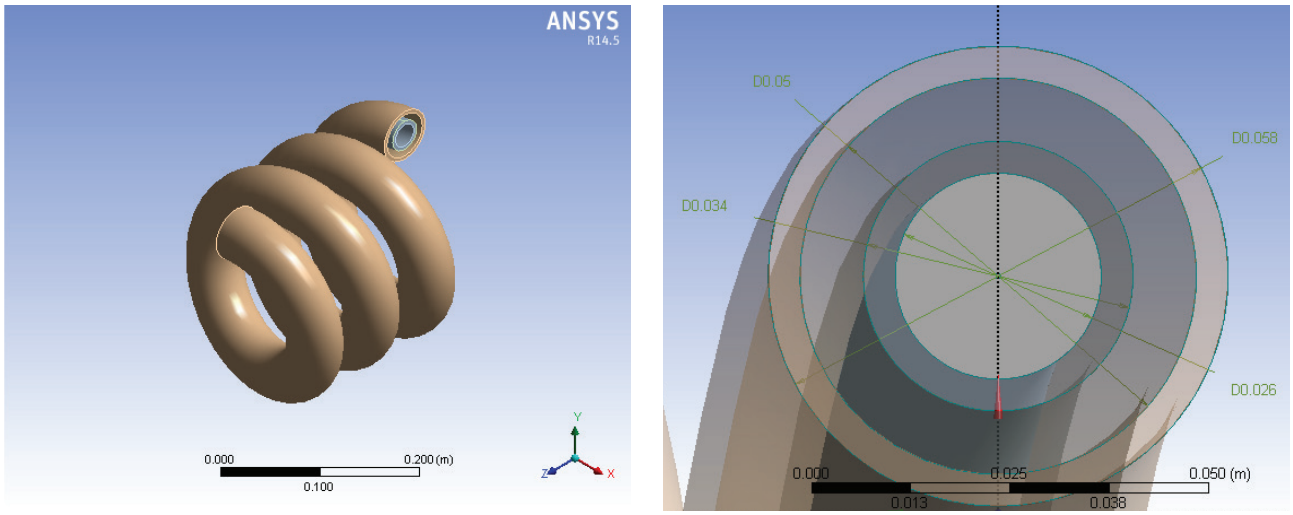

(a) 3 – D model (b) Close up view of entrance

Figure 4. 3 – D model of the double pipe helical heat exchanger.

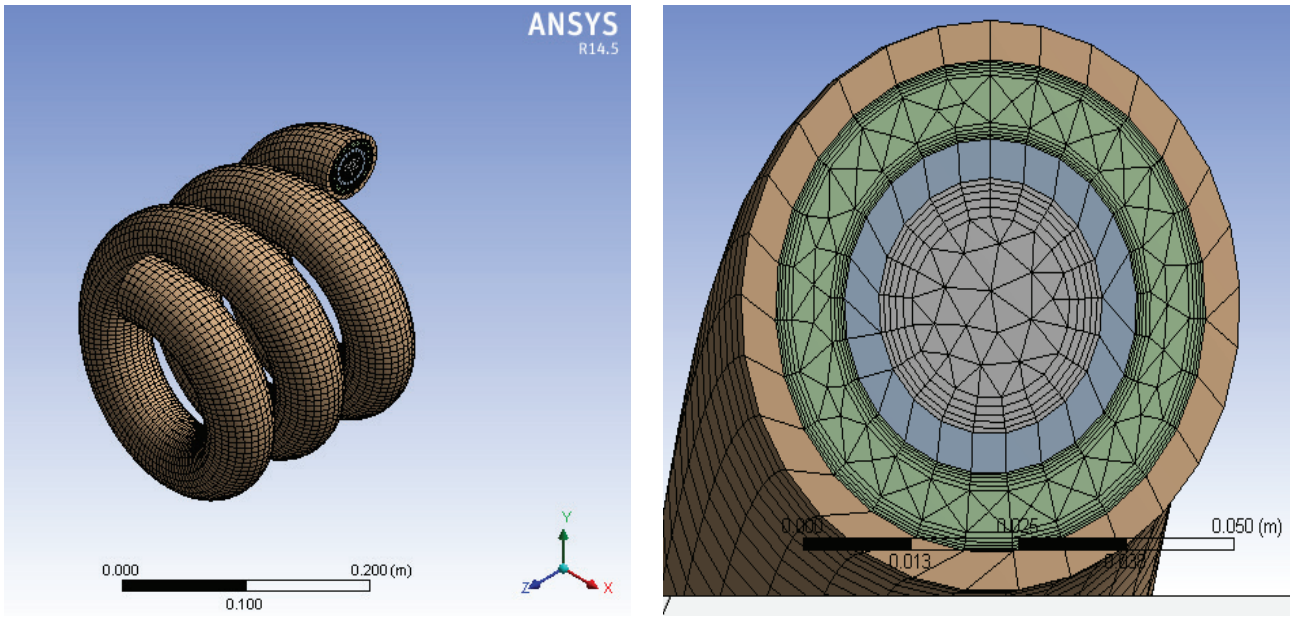

(a) Mesh of helical heat exchanger (b) Mesh of close up view of entrance

Figure 5. Mesh of the computational domain.

Table 4. Mesh metric

Mesh metric	Value
Number of nodes	245659
Number of elements	503877
Element quality	0.612
Aspect ratio	5.387
Skewness	0.238
Orthogonal quality	0.843

and elements in the mesh as well as average values of mesh metric

Figure 6 shows the graph of scaled residuals, as seen a convergence criteria of 10^{-2} was attained.

Figure 7 shows the contours of static temperature for the fluid in the inner pipe (Strong solution of lithium bromide), which is the hot fluid. It can be observed from the figure that there is a progressive loss in temperature of the fluid from entry (top) to exit (bottom) of the heat exchanger. This indicates heat loss to the fluid in the annulus. The hot

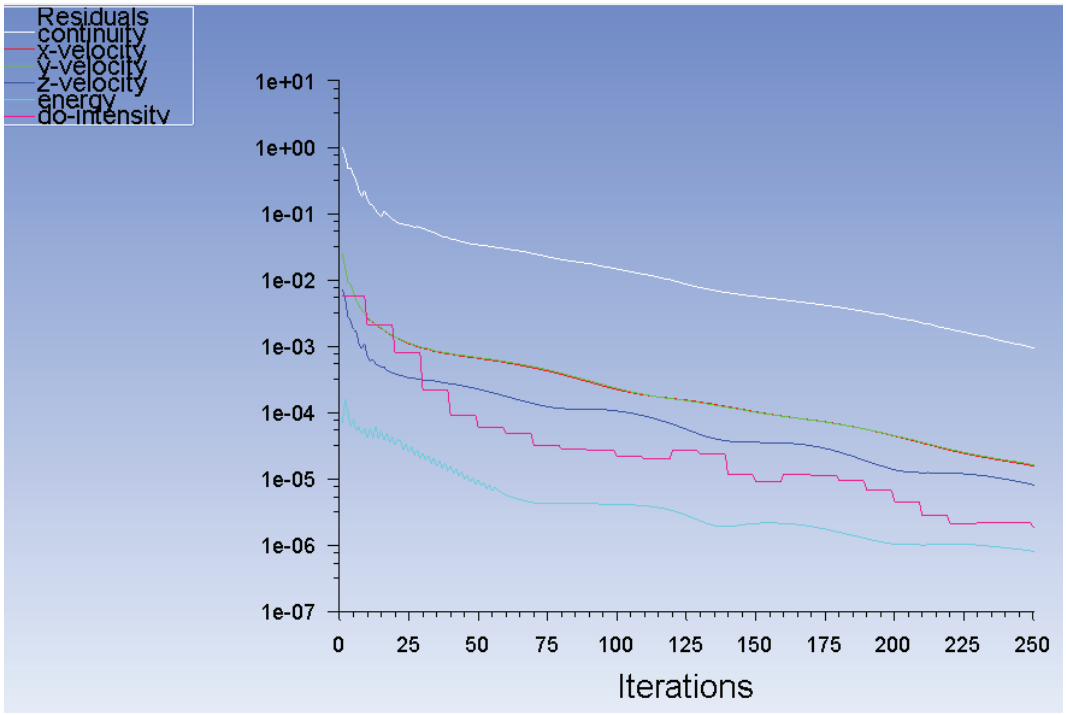

Figure 6. Scaled residuals.

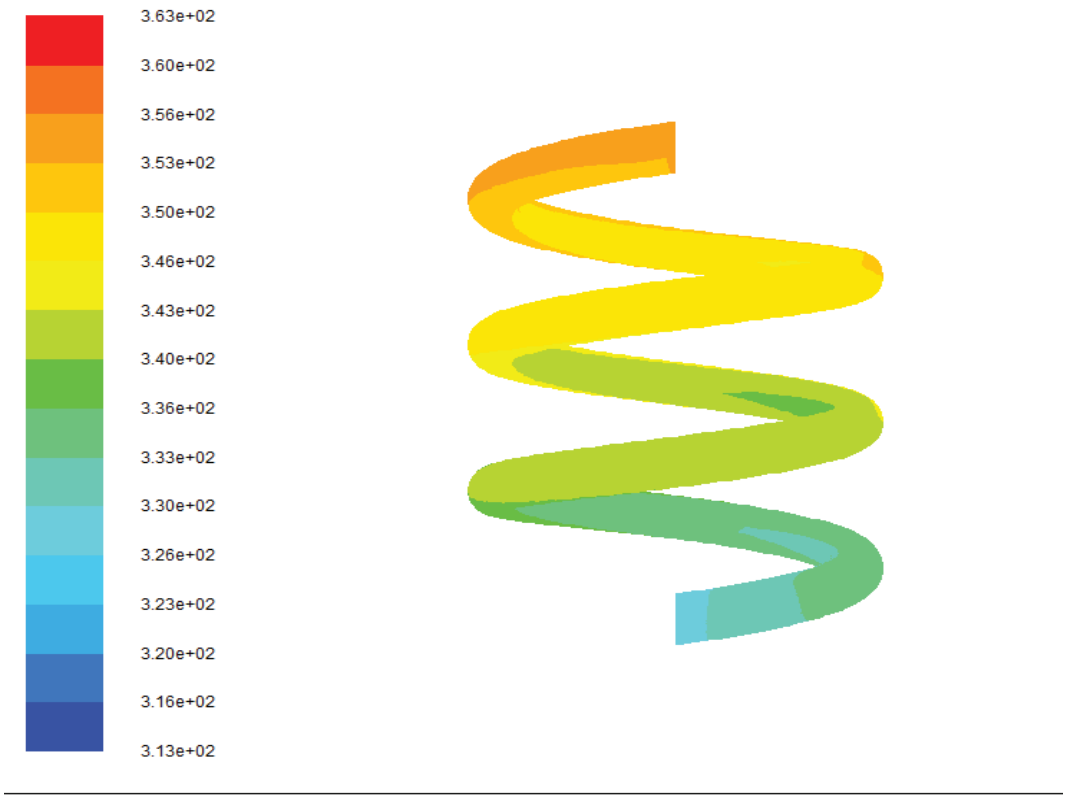

Figure 7. Contours of static temperature for the inner pipe fluid.

fluid with an inlet temperature of 363K (90°C), finally exits the heat exchanger at a temperature of 330K (57°C). This indicates that the desired reduction in temperature of the strong solution at exit from the heat exchanger has been achieved.

Figure 8 shows the contours of static temperature for the fluid in the outer pipe (weak solution of lithium bromide), which is the cold fluid. As seen from the contours, there is a progressive rise in temperature of the fluid from inlet (bottom) to exit (top) of the heat exchanger. This indicates heat transfer from the fluid in the inner pipe to the fluid in the annulus. The fluid with an inlet temperature of 313K (40°C), finally exits the heat exchanger at a temperature of 340K (67°C). This indicates that the desired increase in temperature of weak solution at exit from the heat exchanger has been achieved.

Figures 9 and 10 show the contours of wall shear stress for the inner pipe and outer pipe respectively. As observed

Figure 8. Contours of static temperature for outer pipe fluid.

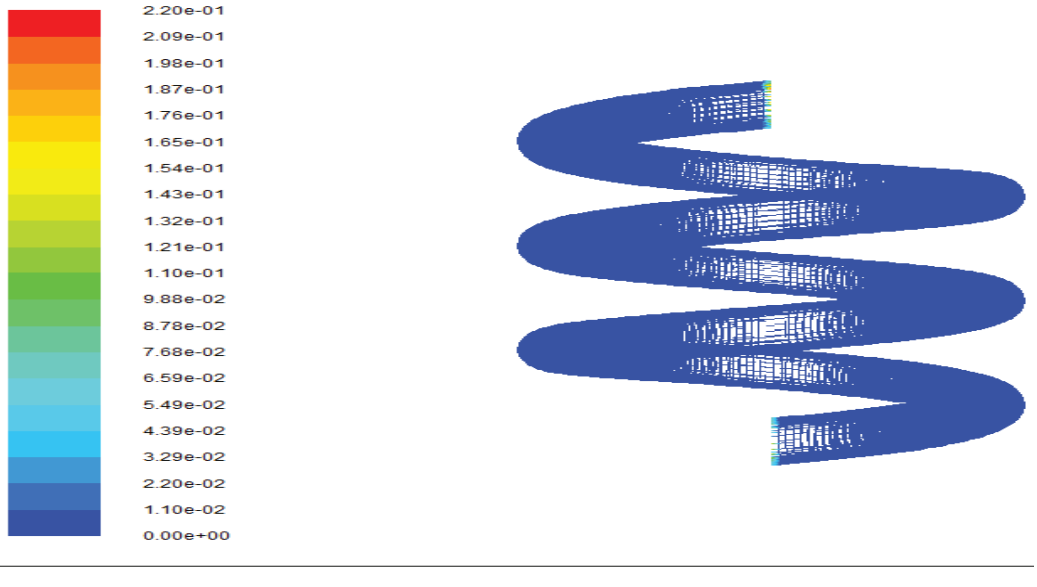

Figure 9. Contours of wall shear stress for the inner pipe.

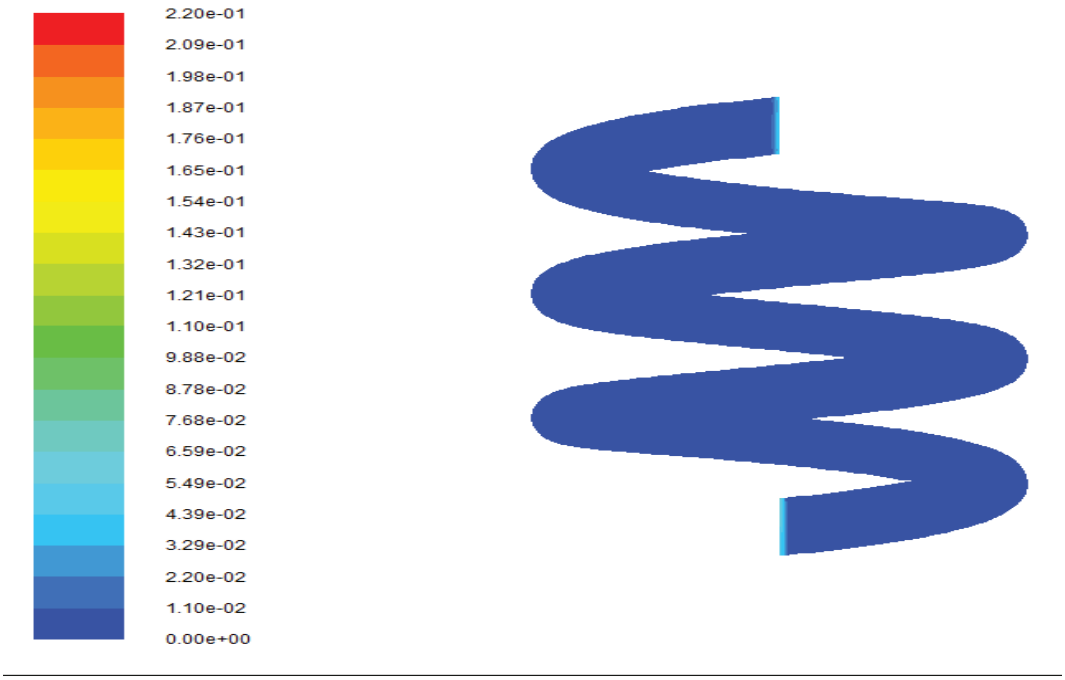

Figure 10. Contours of wall shear stress for the outer pipe.

from both figures, the wall shear stress on both inner and outer pipe is 0.011Pa, though at the tip of the pipes, wall shear stress of 0.0659Pa can be seen. However, on comparing with the mechanical properties of the thermally enhanced polymeric material as shown in table 1, the tensile strength for the material is 103.4 MPa. This indicates that the wall shear stress on both pipes is well within safe limits.

Figure 11 shows the temperature profile of the hot fluid (strong lithium bromide solution) and cold fluid (weak lithium bromide solution) at different points in the polymer heat exchanger from inlet to exit in a counter flow arrangement. As observed from the figure, there is progressive

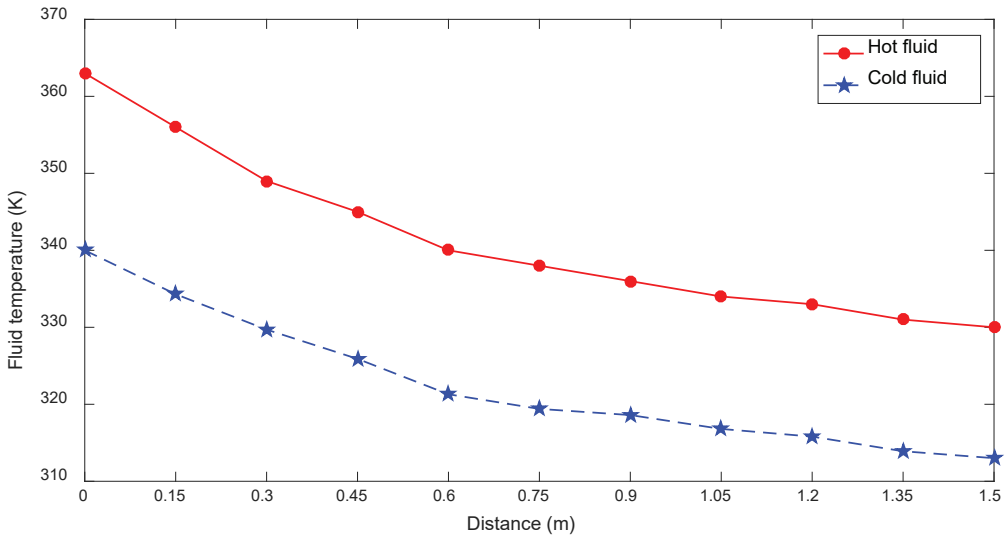

Figure 11. Temperature profile of hot and cold fluid in polymer heat exchanger.

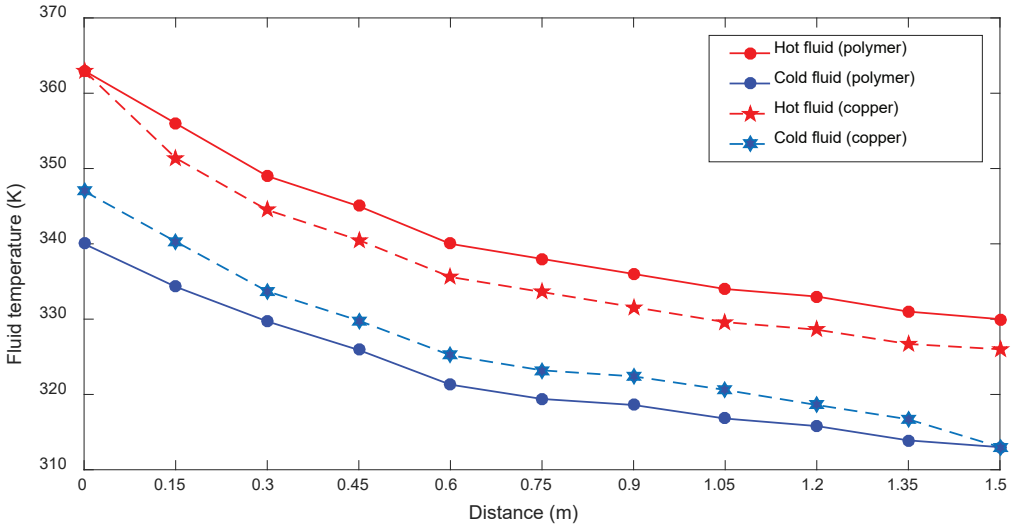

Figure 12. Comparison of temperature profiles of fluids in polymer heat exchanger with fluids in copper heat exchanger.

decrease in temperature of the hot fluid from inlet to exit (left to right), while the cold fluid increases in temperature from inlet to exit (right to left). This is an indication of heat transfer between the two fluids across the walls of the heat exchanger. The hot fluid inlet and exit temperatures are 363K (90°C) and 330K (57°C) respectively, while the cold fluid inlet and exit temperatures are 313K (40°C) and 340K (67°C) respectively. This indicates the heat exchanger has been able to carry out the required duty.

Figure 12 shows the temperature profile of hot and cold fluids at different points in the polymer heat exchanger in comparison to the temperature profile of hot and cold fluids at the same points in a copper heat exchanger. The copper heat exchanger was modelled using the same geometric parameters and flow conditions as the polymer heat exchanger. As observed from the figure, hot fluid in both heat exchangers experience a progressive loss in temperature from inlet to exit, while the cold fluid in both heat exchangers experience increase in temperature from inlet to outlet. However, hot fluid temperatures in the copper heat exchanger are lower than those of polymer heat exchanger at corresponding points. Similarly, cold fluid temperatures in the copper heat exchanger are higher than those of polymer heat exchanger at corresponding points. It can be observed from the figure that the hot fluid outlet temperatures are 330K (57°C) and 326K (53°C) for the polymer and copper heat exchangers respectively. While the cold fluid outlet temperatures are 340K (67°C) and 347K (74°C) for the polymer and copper heat exchangers respectively. This indicates higher heat flux in copper heat exchanger in comparison to the polymer heat exchanger.

The effectiveness of the polymer and copper heat exchangers were computed using equation 7, together with the inlet and outlet fluid temperatures of both heat exchangers. The effectiveness of the polymer heat exchanger was obtained as 77.4%, while the effectiveness of the copper heat exchanger was obtained as 86.8%. This is close to the effectiveness of 0.84 – 0.9 obtained by [11] for a helical heat exchanger working on the Ammonia – water pair. This indicates that the proposed polymer heat exchanger could perform the required solution heat exchanger duty 89.2% as effective as the conventional copper heat exchanger. Thus, the prospect of using a helical heat exchanger made from polymer material seems bright.

CONCLUSION

Numerical study of a double pipe helical heat exchanger designed for use as a solution heat exchanger in an absorption chiller of 3 kW capacity has been carried out. A thermally enhanced polymer material made from liquid crystal polymer and carbon fibre was selected as the material for the heat exchanger. Numerical study of heat transfer in the heat exchanger was done with the numerical software ANSYS fluent version 14.5. Results indicate that the heat exchanger was able to carry out the required duty of heat transfer between the hot and cold lithium bromide solutions. Results indicate that the polymer heat exchanger attained an effectiveness of 77.4%. This translates to 89.2% of the effectiveness of a corresponding heat exchanger using copper material. With this, the prospect of using the studied polymer material as solution heat exchanger in absorption chiller is bright.

NOMENCLATURE

A Heat transfer area, m^2
C Heat capacity rate, W/K
C_p Specific heat, J/kg.K
D Tube diameter, m
De Dean number
D_h Hydraulic diameter, m
E Total energy, J
F External body force, N
$\vec{j}_j$ Diffusion flux, $mol/m^2.s$
K_{eff} Effective conductivity, W/m.K
$\dot{m}$ Mass flow rate, kg/s
p Pressure, N/m^2
q Rate of heat transfer, W
r Tube radius, m
R_c Coil radius, m
Re Reynolds number
Re_{crit} Critical Reynolds number
S_h Heat of chemical reaction, kJ/mol
T Temperature, K
ΔT_{lm} Log mean temperature difference
U Overall heat transfer coefficient, W/m^2K
v Fluid velocity, m/s
v Velocity field, m/s

Greek symbols
Δ Increment
ε Effectiveness
ρ Density, kg/m^3
ρg Gravitational body force, N
μ Fluid dynamic viscosity, $N.s/m^2$
$\bar{\bar{\tau}}$ Stress tensor, N/m^2

Subscripts
c Cold fluid
eff Effective
h Hot fluid
i Inlet
o Outlet
max Maximum
min Minimum

AUTHORSHIP CONTRIBUTIONS

Authors equally contributed to this work.

DATA AVAILABILITY STATEMENT

The authors confirm that the data that supports the findings of this study are available within the article. Raw data that support the finding of this study are available from the corresponding author, upon reasonable request.

CONFLICT OF INTEREST

The author declared no potential conflicts of interest with respect to the research, authorship, and/or publication of this article.

ETHICS

There are no ethical issues with the publication of this manuscript.

REFERENCES

[1] Theodore LB, Adrienne SL, Frank PI, David PD. Fundamentals of heat and mass transfer. 7th ed. New York: John Wiley & Sons; 2011.
[2] Estiot E, Natzer S, Schweigler C. Heat exchanger development for compact water/LiBr Absorption systems. Proceedings of the 22nd International Congress of Refrigeration, Beijing. 2007; 5572−5582. [CrossRef]
[3] Kurnia JC, Ghoreishi-Madiseh SA, Sasmito AP. Heat transfer and entropy generation in concentric/eccentric double-pipe helical heat exchangers. Heat Transf Eng 2020;41:1552−1575. [CrossRef]
[4] Cevallos JG, Bergles AE, Bar-Cohen A, Rodgers P, Gupta SK. Polymer heat exchangers - history, opportunities and challenges. Heat Transf Eng 2012;33:1075-1093. [CrossRef]
[5] Wharry Jr SR. Fluoropolymer heat exchangers. Met Finish 1999;97:769−781. [CrossRef]
[6] Arie MA, Tiwari R, Shooshtari AH, Dessiatoun SV, Ohadi MM, Pearce JM. Experimental characterization of heat transfer an additively manufactured polymer heat exchanger. Appl Therm Eng 2017;113:575−584. [CrossRef]
[7] Xu S, Liu J, Wang X. Thermal conductivity enhancement of polymers via structure tailoring. J Enhanc Heat Transf 2020;27:463−489. [CrossRef]
[8] Bar-Cohen A, Rodgers P, Cevallos J, Luckow P. Application of thermally enhanced plastics to sea water cooled applications. Proceedings of the Second International Energy 2030 Conference, Abu Dhabi, 2008.
[9] Rennie TJ, Raghavan VG. Experimental studies of a double pipe helical heat exchanger. Exp Therm Fluid Sci 2005;29:919−924. [CrossRef]
[10] Rennie TJ, Raghavan VG. Numerical studies of a double pipe helical heat exchanger. Appl Therm Eng 2006;26:1266−1273. [CrossRef]
[11] Ramesh R. Murugesan S. N. Narendran C. and Saravanan R. 2017. Experimental investigation on shell and helical coil solution heat exchanger in ammonia - water vapour absorption refrigeration system. Int Commun Heat Mass Transf 2017;87:6−13. [CrossRef]
[12] Mohammed FA, Dhafer AH, Mushtaq EA. Experimental and CFD analysis of heat transfer in a double pipe helical coil heat exchanger. Int J Mech Prod Eng Res Dev 2018;8:991−1000. [CrossRef]
[13] Maisari M, Valipour MA, Arasteh H, Toghraie D. Energy and exergy analysis and optimization of helically grooved shell and tube heat exchangersby using Taguchi experimental design. J Therm Anal Calorim 2020;139:3151−3164. [CrossRef]

[14] Han Y, Wang XS, Zhang HN, Chen QZ, Zhang Z. Multi - objective optimization of helically coiled tube heat exchanger based on entropy generation theory. Int J Therm Sci 2020;147:106150. [CrossRef]
[15] Prerana N, Thokchom SS, Upendra R, Tikendra NV. Effect of Dean number on the heat transfer characteristics of a helical coil tube with variable velocity and pressure inlet. J Therm Eng 2020;6:128−139. [CrossRef]
[16] Li Y, Wu J, Wang H, Kou L, Tian X. Fluid flow and heat transfer characteristics in helical tubes cooperating with spiral corrugation. International conference on future electrical power and energy systems. Energy Procedia 2012;17:791−800. [CrossRef]
[17] Sobota T. Experimental and numerical analysis of heat transfer in the helically coiled heat exchanger. Int J Numer Method Heat Fluid Flow 2020;30:2935−2951. [CrossRef]
[18] Srinivasan, S., Nadapurkar, S. and Holland, F. A. Friction factor for coils. Trans Inst Chem Eng 1970;48:156−161.
[19] ANSYS. ANSYS Fluent Users Guide. V.14.5 User Manual. 2013.
[20] McNeely LA. Thermodynamic properties of aqueous solutions of lithium bromide. ASHRAE Trans 1979;85:413−434.